*Geotechnical Testing Journal*, Vol. 29, No. 5
Paper ID GTJ100024
Available online at: www.astm.org

*Wenjun Dong*[1] *and A. P. S. Selvadurai*[2]

# Image Processing Technique for Determining the Concentration of a Chemical in a Fluid-Saturated Porous Medium

**ABSTRACT:** This paper presents a color visualization-based image processing technique for the quantitative determination of a chemical dye concentration in a fluid-saturated porous column composed of glass beads. In this image processing technique, an image filter is designed by taking into account the porous structure of the medium and color characteristics of both the fluid and the solid particles to extract the color representation of the dye solution in pore space, which enables the image quantification. A comparison of experimental results with analytical and numerical simulations illustrates the efficiency and accuracy of the image processing method for determining the chemical concentrations in the porous medium.

**KEYWORDS:** image processing, image filtering, image quantification, truecolor image, transport in porous column, analytical and numerical simulations

## Introduction

Experimental work is an important aspect of environmental geosciences both for the verification of theoretical models and for the identification of parameters governing physical phenomena. A key aspect of experimentation associated with the transport of a chemical through a porous medium relates to the measurement of the chemical concentration within the pore space. An important constraint on such measurements is that the procedure should be noninvasive. Any measuring device or a probe placed within the porous medium (Bear 1961; Robbins 1989) would act as an anomaly that would influence the flow and transport process in the porous medium. With the advent of efficient technologies for visualization and processing of digital data, imaging techniques have been successfully applied in a number of areas in the pure and applied sciences and they have become important tools for data analysis in geomechanics and geoenvironmental engineering (Allersma 1990; Dawe et al. 1992; Carunan and Dawe 1996; Macari et al. 1997; Garboci et al. 1999; Asundi 2002; Rechenmacher and Finno 2004).

Recent advances in image analysis offer great potential for the accurate and effective determination of solute transport in porous media, and several image-based techniques have been developed for this purpose. These include x-ray tomography (Warner et al. 1989), positron emission tomography (Park and McNeil 1996; Khalili et al. 1998), photoluminescent volumetric imaging (Montemagno and Gray 1995), nuclear magnetic resonance imaging (Majors et al. 1991; Shattuck et al. 1997; Grenier et al. 1997) and color visualization-based image processing (Corapcioglu and Fedirchuk 1999; Huang et al. 2002).

Manuscript received September 16, 2005; accepted for publication April 25, 2006; published online June 2006.

[1]Graduate student, Department of Civil Engineering and Applied Mechanics, McGill University, 817 Sherbrooke Street West, Montreal, QC, Canada H3A 2K6.

[2]Corresponding author, William Scott Professor and James McGill Professor, Department of Civil Engineering and Applied Mechanics, McGill University, 817 Sherbrooke Street West, Montreal, QC, Canada H3A 2K6, e-mail: patrick.selvadurai@mcgill.ca

Since the color visualization-based image processing method is noninvasive and easy to implement, the procedure has been recently used to quantify the solute transport process in the idealized porous medium. Corapcioglu et al. (1997) and Corapcioglu and Fedirchuk (1999) employed the dye visualization technique to quantify the solute transport with a glass-etched micromodel and a glass bead micromodel. Huang et al. (2002) used the fluorescent dye tracer excited by a background ultraviolet light source to examine the solute transport processes in an idealized porous layer of nominal thickness consisting of translucent glass beads. Theodoropoulou et al. (2003) measured the solute dispersion on artificial etched planar pore networks based on the detection of color changes of the solution caused by a variation in pH. In these applications, the solute concentration profile was determined according to the imaged color intensity recorded by a CCD digital camera. Since the color variation was illuminated by a transmitted light source placed beneath the sample, these methodologies introduce light dispersion effects that can influence the accuracy of quantitative evaluations of the experimental results (Huang et al. 2002).

This paper presents a color visualization-based image processing method for the quantitative determination of the chemical dye concentration in a fluid-saturated porous medium. In order to avoid the dispersion of light by the glass beads, a strong diffusive light source is applied to front of sample. An image filtering procedure is developed to remove the image noise resulting from the reflection of light by the glass spheres. Such an image filtering procedure, designed on the basis of the porous structure and color characteristics of both the pore fluid and the solid particle, is used to extract the color representation of the chemical solution in the pore space. The color intensity is then used to quantify the chemical concentration. The quantitative distributions of the concentration of the dye solution obtained from the image processing method are used to estimate the hydrodynamic dispersion coefficient, which can be used in analytical and numerical models for examining the chemical concentration. Finally the experimental results of the transport of a dye solution measured in the visible interface between the glass tube and porous medium are compared with the analytical and nu-

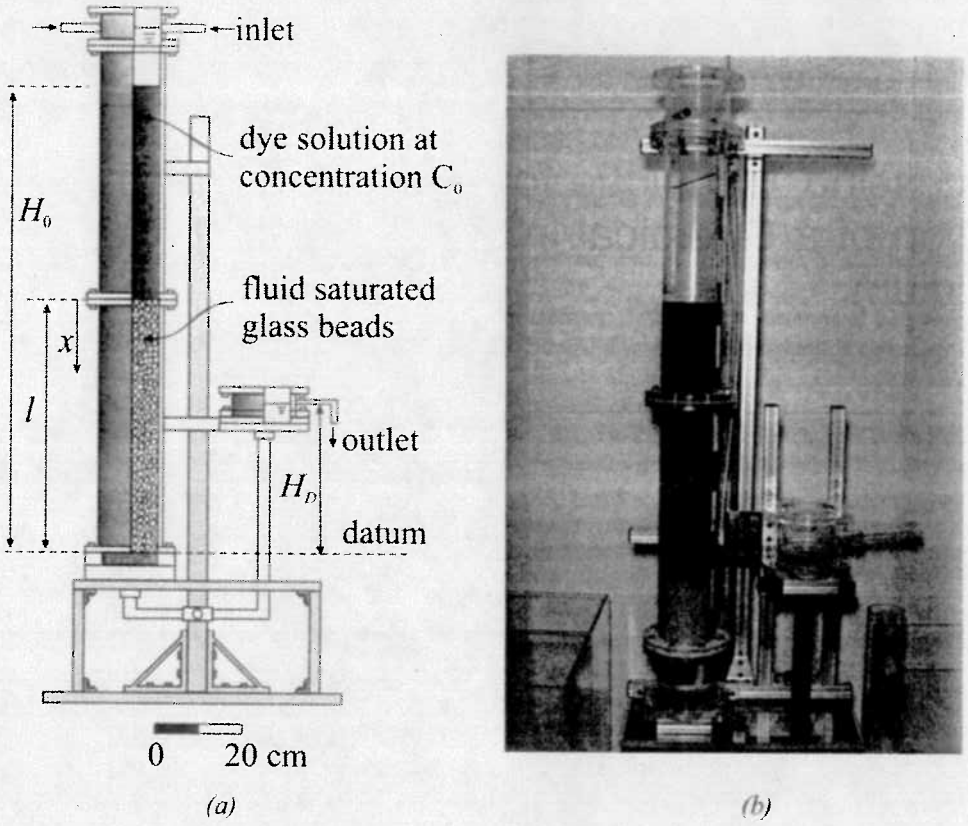


FIG. 1—*The schematic (a) and photographic (b) views of experimental configuration of column apparatus.*

merical solutions, to illustrate the efficiency and accuracy of the image processing method.

## Experimental Design

The schematic and photographic views of the experimental configuration used to study the movement of a chemical dye solution in an idealized porous column are shown in Fig. 1. The apparatus consisted of a series of precision-manufactured smooth-walled glass cylinders of internal diameter 15 cm, length 61 cm, and wall thickness 0.50 cm that were connected to form a one-dimensional column of length 102 cm. The use of precision glass cylinders minimizes damage due to abrasion of the interior surface and provides a relatively distortion-free transparent surface for observation of the chemical migration pattern. The porous medium consisted of a packed bed of glass spheres (of specific gravity approximately 2.5) with the sizes ranging from 150–212 μm. The glass beads were placed to a height of 61 cm in a column of water to a porosity of approximately 38.5 %. The hydraulic conductivity $k$ of the porous column was measured by conducting conventional falling head tests, and the measured value was $k = 2.05 \times 10^{-4}$ m/s. A water-soluble *sodium chloride acid red dye* mixed with water was used as the dye solution with a concentration of 1 g/l. This dye solution was placed above the porous column and used as the tracer to illustrate the chemical migration pattern in the visible region of the porous column. Careful placement of the dye solution was necessary to eliminate the premature migration of the chemical dye solution into the porous region. As a result, the porous medium section of the column was regarded as free of any chemical dye. Furthermore, since the preparation time for the experiment was relatively small, any diffusion of the dye solution into the saturated porous medium was also be neglected. The transport of the dye solution through the porous column was initiated by a hydraulic gradient across the porous column.

The transport process of the dye solution at the cylindrical interface between the glass tube and the porous medium was recorded at specific time intervals using a CCD camera. A strong diffusive light placed in front of the column was used to eliminate any influence of ambient lighting. The digital camera was positioned at front of the porous column and at the midpoint level of the spatial range of interest, and its settings such as the shutter speed, aperture, and white balance determined by the condition of the diffusive lighting, were maintained constant for all experiments, including in the calibration exercises. An image strip, which is approximately 60 cm long (915 pixels) and 1.5 cm wide (20 pixels), was extracted from the photographic image along the central part of porous column for purposes of determining the concentration of the dye solution along the visible cylindrical surface of the test column. Since the diameter of the glass tube was much greater than the width of narrow strip, any influence of light distortion due to the curvature of the glass tube was neglected in the image analysis of the chosen strip region.

## Image Filtering Procedure

The visual image of the migration of the dye solution through the porous column, recorded by the digital camera, contains not only the color of the fluids in the pore space (i.e., either the chemical dye solution in dye-dosed zone or water in water-saturated zone), but also the color of glass beads adjacent to the cylindrical surface of

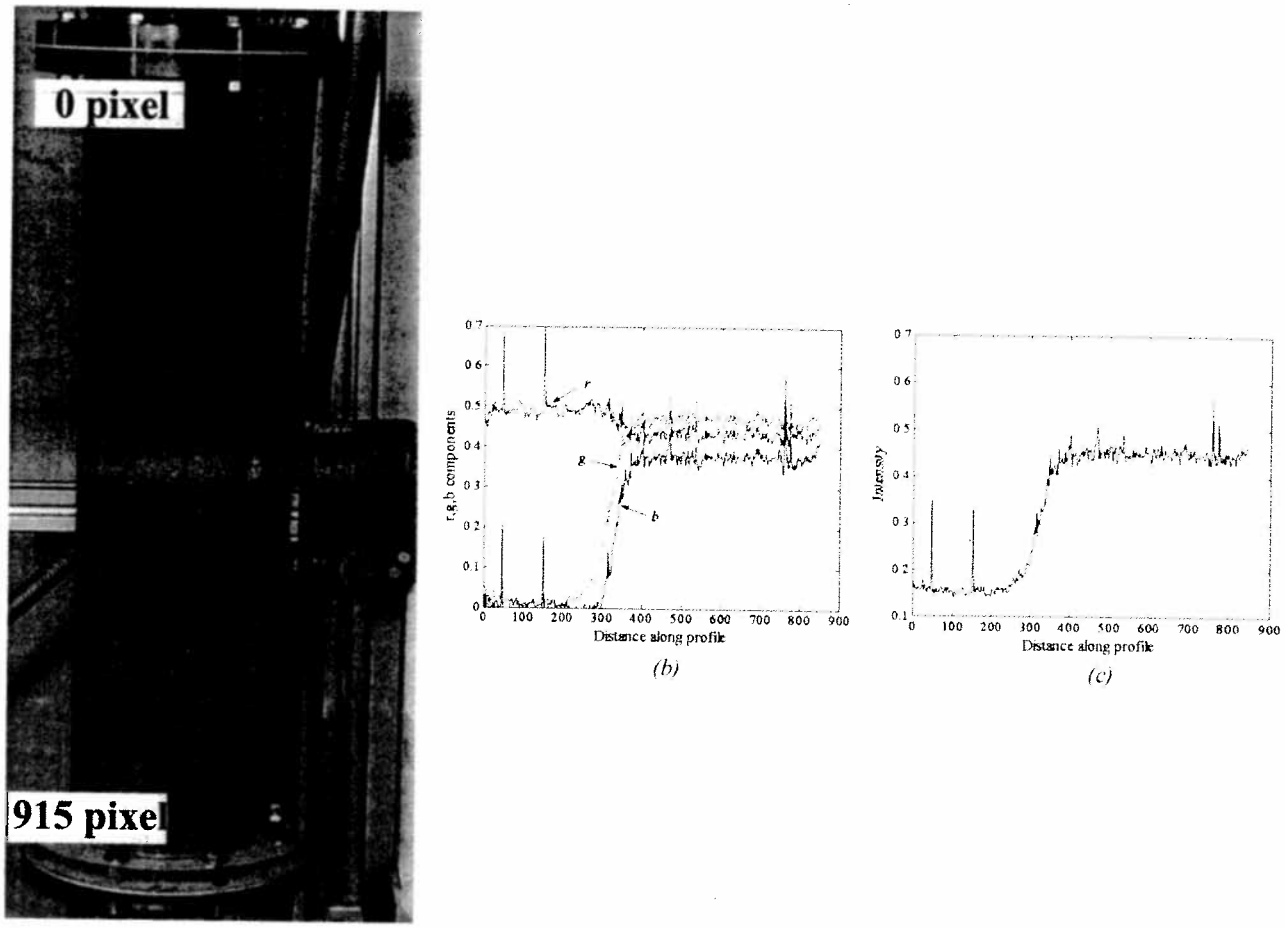


(a) (b) (c)

FIG. 2—*The distribution of the r, g, b color components and the intensity along the vertical profile line. (a) an original image, (b) r, g, b color components, and (c) intensity.*

the column. Only the color representation of the fluids in the pore space should be considered for purposes of an image analysis. In order to obtain the color distribution of the dye solution of different concentrations in the pore space, the image can be enhanced by interpreting the color of glass beads as noise imposed on the color of the pore fluids and by extracting it from the image.

The realistic area porosity on the surface between the glass tube and the glass bead column is larger than the volumetric porosity of the column that is 38.5 % (Garboci et al. 1999). For assemblies of glass spheres, the theoretical estimates for the area porosity on the surface of glass beads can range from 47.5 % for a cubic packing to 26 % for a hexagonal packing (Corapcioglu and Fedirchuk, 1999). Therefore, it can be assumed that area porosity of a region at the interface between the glass tube and the porous column is close to 40 %. Therefore, it can be concluded that approximately 40 % of pixels in an image of the sample contains the color representing the pore fluids in pore space and 60 % of pixels contains the color contribution from glass beads. Furthermore, since an image of a strip of a width 1.5 cm and length 60 cm contains 915 pixels in length, a 5 by 5 pixel neighborhood in the image strip should correspond to a 1 cm by 1 cm area on the cylindrical surface of the glass bead column, the size of which is about 50 to 70 times of the diameter of the glass bead. Such 1 cm by 1 cm area can be considered as a Representative Elemental Volume on the surface of the glass bead column. Therefore, it can be concluded that for a 5 by 5 pixel neighborhood in the image strip, on average, 10 out of 25 pixels (i.e., 40 %) contain the color representing the dye solution in the pore space.

The photographic records captured by the digital camera are *truecolor* images in the form of two-dimensional digital arrays of pixels. The truecolor image at each pixel consists of the three primary colors, red, green, and blue $(r,g,b)$, and it can be transformed from the RGB color space into the color space expressed in terms of the Hue, Saturation, and Intensity (Russ 1994). The intensity $I$ is defined as $I=(r+g+b)/3$ and it can reflect the color variation in the gray scale. For example, for the typical image shown in Fig. 2(*a*), the variation in the RGB color components along a vertical line at the center of the column are shown in Fig. 2(*b*) and the corresponding profile of the intensity along this vertical line is shown in Fig. 2(*c*). It may be noted from Fig. 2(*b*) that the red color component in both the dye-dosed and water-saturated zones in the image is almost uniformly distributed. The green and blue color components, however, vary significantly in these zones, resulting in a low intensity in dye-dosed zone and a high intensity in water-saturated zone. This variation of the intensity can also be observed in Fig. 2(*c*). The oscillations in the intensity profile correspond to the color noise resulting from light reflection from the glass spheres adjacent to the surface of the column. In general, due to the light reflection, the intensity of the glass spheres is lower than that of the ambient solutions in both the dye-dosed and water-saturated zones. Therefore, if

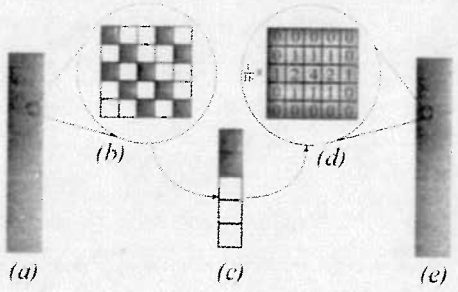


FIG. 3—*The image filtering procedure, (a) an original image, (b) schematic view of the 5 x 5 pixel neighborhood taken from the original image, (c) the ordered color set of the neighborhood in the intensity increment, (d) the color redistribution of the 5 x 5 pixel array and the weighting kernel, and (e) the enhanced image.*

25 pixels in the above 5 by 5 pixel array taken from the dye-dosed zone are sorted in terms of the intensity increment, then the upper ten elements in the ordered set will contain the color representing the dye solution in the pore space and remaining 15 elements will contain the color contribution from the glass spheres. A similar result can be obtained for the neighborhood of the 5 by 5 pixel array taken from the water-saturated zone in the image since the intensity for the water in the pore space is also higher than that for the glass spheres in the contact region. A median of the upper ten elements of the ordered color set was chosen to replace the color at the central pixel in the 5 by 5 pixel neighborhood. Hence, if the color at this central pixel corresponded to a glass sphere, it would then be replaced by the color of its ambient fluids using the procedure just described. This approach is also referred to as *order-statistics filtering* (Gonzalesz and Woods 2002). The color representation of the glass beads can be removed from the image by applying the order-statistics filtering to each pixel in the image. After application of the order statistics procedure, a *linear spatial filtering procedure* is applied to smooth the image by means of a weighted averaging of the color value at a pixel with the ones at its neighboring 24 pixels. In this procedure, the value at the central pixel in the 5 by 5 neighborhood was replaced by the weighted average of the 25 elements of the 5 by 5 array.

Figure 3 shows a schematic illustration of the image filtering procedure. The image strip shown in Fig. 3(*a*) was extracted from the photographic record contained in Fig. 2(*a*). Some white spots can be observed in both the dye-dosed and water-saturated zones in the image due to reflection of light from certain glass spheres adjacent to the surface of the porous column. These reflection spots correspond to large oscillations in the intensity profile shown in Fig. 2(*b*) and they could be removed by using the image filtering procedure described previously. A schematic diagram of the image neighborhood of a 5 by 5 pixel array isolated from original image is shown in Fig. 3(*b*). This 5 by 5 image array is sorted in terms of the intensity increment (Fig. 3(*c*)). The color median of the upper ten elements in the ordered set was then chosen to replace the color at the central pixel of the 5 by 5 pixel array. A linear smoothing filtering procedure was then applied to the image with the weighted kernel shown in Fig. 3(*d*). The final enhanced image shown in Fig. 3(*e*) contains a noise-free color distribution.

## Image Quantification

For purposes of the image quantification, preliminary tests should be performed to calibrate the concentration level of the chemical

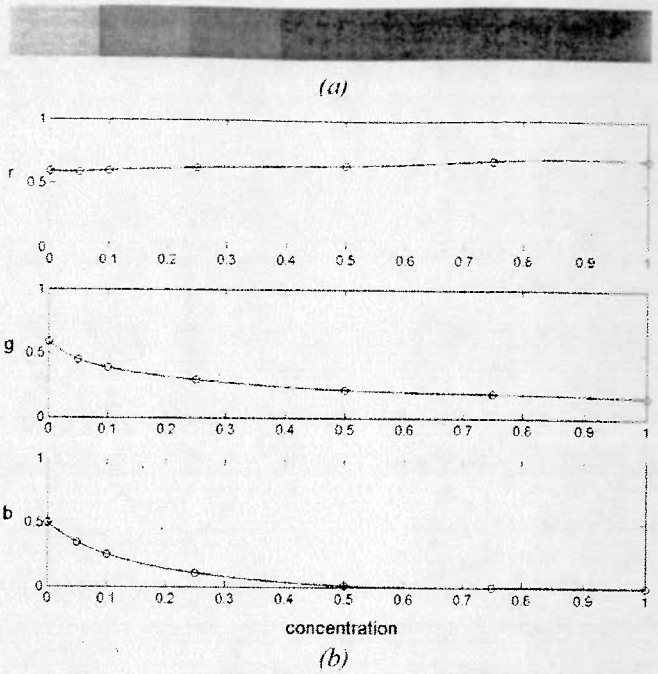


FIG. 4—*(a) The enhanced images of the seven calibration samples and (b) the cubic spline fitting curves of the three color components.*

dye solution in its in situ condition within the porous column. In the preliminary calibration tests, the glass beads were placed to the reference porosity in seven dye solutions of known concentrations, ranging from 0, 0.05, 0.1, 0.25, 0.5, 0.75, to 1.0 g/l, to develop a relationship between the concentrations of the dye solution and their color counterparts within the porous column. The narrow image strips were extracted from the photographic records along the porous column to make seven color image samples. These image samples were enhanced to extract the color representations of the dye solution in the pore space by using the image filtering procedure described previously.

The enhanced images corresponding to different dye concentrations in the pore space of the porous column shown in Fig. 4(*a*) indicate that the color images vary with the concentration of the chemical dye solution in the porous medium. These color images can therefore be used as the database for interpreting the concentration of the dye solution in the porous column, and they represent *seven points* in the plane of the concentration of the dye solution *versus*. the composition of each of the primary color components *red*, green and *blue* (Fig. 4(*b*)). A *cubic spline interpolation* can be applied to these sample points to generate the smooth polynomial curves for each primary color component (Fig. 4(*b*)). These interpolating curves represent a mapping between the concentration of the dye solution and its color counterpart in the pore space, and they were used as the reference to convert the color distribution to a quantitative estimate of the dye concentration in pore space of the porous column.

It should be noted that the color-concentration mapping used to quantify the images is defined on a color set $G$ created by the interpolating curves of seven calibration samples shown in Fig. 3(*b*). The observed color $(r_{ij}^{ob}, g_{ij}^{ob}, b_{ij}^{ob})$ at a certain pixel $(i,j)$ in the image of the migration of the dye solution through the porous column (i.e., captured by a digital camera and enhanced by the image filtering procedure), however, may not necessarily belong to the color set $G$ (i.e., $(r_{ij}^{ob}, g_{ij}^{ob}, b_{ij}^{ob}) \notin G$). This can be due to errors intro-

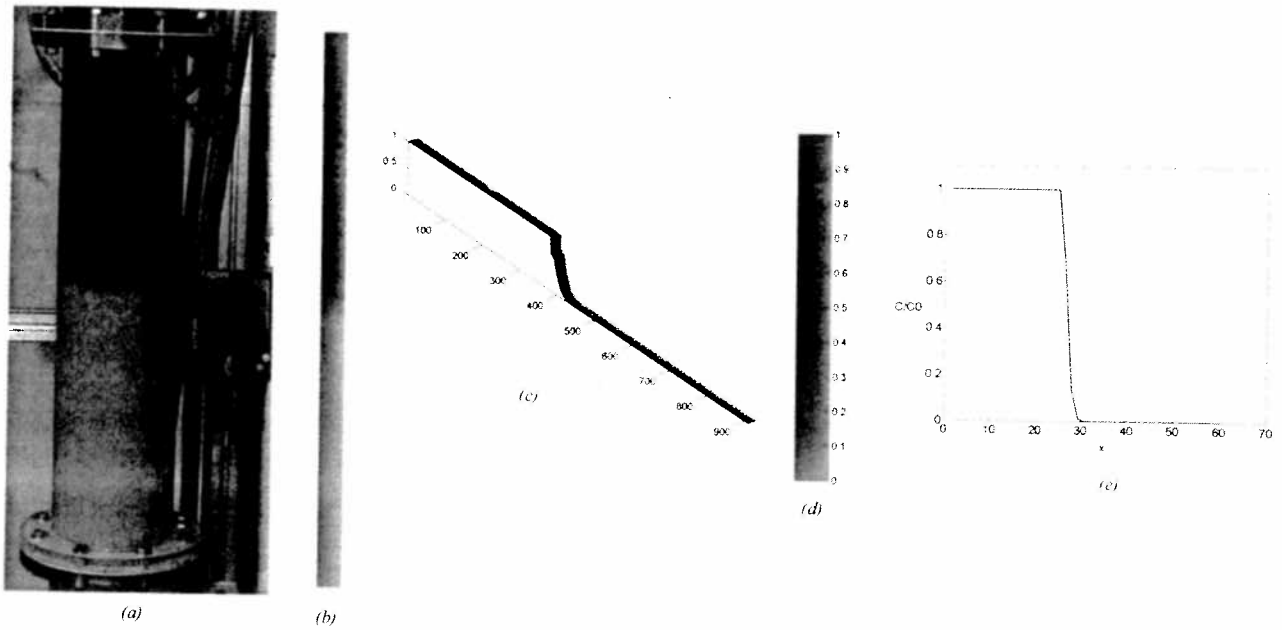


FIG. 5—*The quantification of the concentration distribution of the dye solution at the cylindrical surface of the porous column, (a) a photographic record, (b) an image strip, (c) the color quantification, (d) the color bar, and (e) the quantitative distribution of the dye concentration.*

duced by the experiment and the image filtering process. Therefore, the projection $(r'_{ij},g'_{ij},b'_{ij})$ of the observed color $(r^{ob}_{ij},g^{ob}_{ij},b^{ob}_{ij})$ in $G$ should be used for the purpose of color quantification at the pixel $(i,j)$ of the image. The projection $(r'_{ij},g'_{ij},b'_{ij})$ in $G$ can be determined from a "shortest distance" concept; i.e.,

$$E(r'_{ij},g'_{ij},b'_{ij}) = \min_{(r,g,b)\in G} E(r,g,b) \tag{1}$$

where $E$ represents a Euclidean norm of $(r^{ob}_{ij},g^{ob}_{ij},b^{ob}_{ij})$ to the color set $G$; i.e.,

$$E(r,g,b) = \sqrt{(r^{ob}_{ij}-r)^2+(g^{ob}_{ij}-g)^2+(b^{ob}_{ij}-b)^2} \tag{2}$$

Substituting $(r'_{ij},g'_{ij},b'_{ij})$ into the color versus concentration mapping determined from the interpolating curves shown in Fig. 4(*b*), the color representation of the concentration of the chemical dye solution at the pixel $(i,j)$ can be quantified as

$$C_{ij} = C(r'_{ij},g'_{ij},b'_{ij}) \tag{3}$$

Figure 5 shows the image quantification procedure used to digitize the color distribution of the concentration of dye solution in the visible pore space during its transport through the porous column. A photographic record of the transport process obtained with the digital camera at a specific time is shown in Fig. 5(*a*). The corresponding enhanced image strip extracted from the central part of the column in the photograph is shown in Fig. 5(*b*). The color equivalent of the concentration profile determined using the procedures described previously is shown in Fig. 5(*c*) and a colorbar is shown in Fig. 5(*d*). Finally, the numerical values for the normalized concentration are shown in Fig. 5(*e*).

## Experimental Results

Applying the image filtering and image quantification procedures described in the previous sections to a sequence of images captured at specified time intervals, the transport process of the dye solution at the visible surface of the porous column can be quantified. Figure 6 shows the quantitative estimates for the normalized dye concentration ($C_0$=1.0 g/l), as a function of dimensionless variables $X=x/l$ versus $T=kt/l$. The dye movement takes place at a constant Darcy flow velocity $v(=k(H_0-H_D)/n^*l)=2.18\times10^{-4}$ m/s, driven by the initial boundary hydraulic potentials $H_0$=0.70 m and $H_D$ =0.45 m applied, respectively, at the inlet and outlet boundaries of the porous column. The steady movement of the dye concentration front can be clearly seen in Fig. 6.

In order to verify that the proposed image processing method gives a reasonable concentration profile, especially in the vicinity of the steep front of the dye concentration, the experimental results are compared with the analytical and numerical simulations of the transport process of the dye solution on the cylindrical surface of the porous column. For purposes of computations, two transport parameters governing the migration of dye solution in the porous column, namely, hydraulic conductivity and hydrodynamic dispersion coefficient, should be determined. The hydraulic conductivity

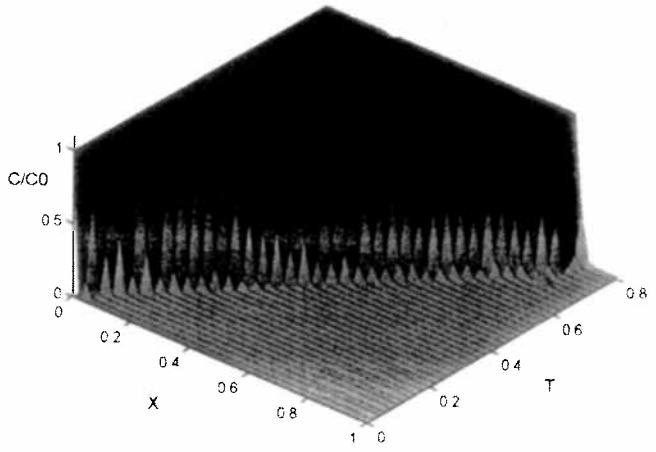


FIG. 6—*The transport process of the chemical dye solution along the cylindrical surface of the glass bead column.*

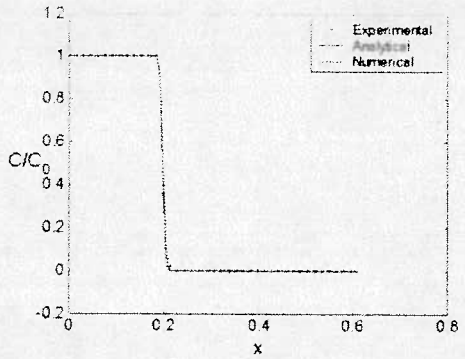


FIG. 7—*The experimental, analytical and numerical solutions for the transport process of the dye solution in the glass bead column at t=360s.*

can be measured by conventional falling head tests and its value was already given in the section dealing with Experimental Design. The determination of hydrodynamic dispersion coefficient for the transport process is less straightforward, but it can be identified by an inverse analysis (Gottlieb and Du Chateau, 1996) in conjunction with the experimental results shown in Fig. 6. By solving an optimization problem generated by an output least-squares technique (Sun, 1994), the hydrodynamic dispersion coefficient corresponding to the transport processes shown in Fig. 6 is estimated at $D = 1.361 \times 10^{-8}$ m$^2$/s. The measured hydraulic conductivity and the identified hydrodynamic dispersion coefficient are substituted into the analytical solution given by Ogata and Banks (1961) and a stabilized computational procedure developed via a modified least-squares scheme (Selvadurai and Dong, 2005) to simulate the transport pattern shown in Fig. 6. Figure 7 shows a comparison of the experimental results for the distribution of the dye solution on the cylindrical surface of the porous column at $t=360$ s with corresponding analytical and numerical solutions. Since the identified transport parameters are used in the analytical solution and numerical modeling, a close correlation can be seen between the concentration profiles for the transport processes obtained experimentally by the image processing method, and the equivalent results obtained through analytical and numerical modeling (Fig. 7).

## Conclusions

In this paper, a color visualization-based image processing method is developed for the quantitative determination of the concentration distribution of a chemical dye solution as it migrates through an idealized porous column consisting of glass beads contained in a glass column. An image filtering procedure is designed to extract the color representation of the pore fluids from the image of the dye distribution for purposes of image quantification. This procedure accounts for the porous structure of the porous medium and the characteristics of the light intensity of both the pore fluids and the glass beads. The close correlation between the concentration profiles determined from the experiments, an analytical solution and a computational scheme indicates the effectiveness and accuracy of the image processing method that is based on a color visualization approach. The image filtering and image quantification procedures proposed in this paper can also be used to determine the two-dimensional transport pattern of a chemical in an accurate way.

*Acknowledgments*

The work described in this paper was supported by a Discovery Grant of the Natural Sciences and Engineering Research Council of Canada, awarded to A.P.S. Selvadurai.

## References

Allersma, H. G. B., 1990, "On Line Measurement of Soil Deformation in Centrifuge Tests by an Image Processing," *9th Int. Conf. on Experimental Mechanics*, Copenhagen, pp. 1739–1748.

Asundi, A. K., 2002, *MATLAB for Photomechanics: A Primer*, Elsevier, Amsterdam, Boston; London.

Bear, J., 1961, "Some Experiments in Dispersion," *J. Geophys. Res.*, Vol. 66, pp. 2455–2267.

Caruana, A. and Dawe, R. A., 1996, "Experimental Studies of the Effects of Heterogeneities on Miscible and Immiscible Flow Processes in Porous Media," *Transport in Chemical Engineering*, Vol. 3, pp. 185–203.

Corapcioglu, M. Y., Chowdhury, S., and Roosevelt, S. E., 1997, "Micromodel Visualization and Quantification of Solute Transport in Porous Media," *Water Resour. Res.*, Vol. 33, pp. 2547–2558.

Corapcioglu, M. Y. and Fedirchuk, P., 1999, "Glass Bead Micromodel Study of Solute Transport," *J. Contam. Hydrol.*, Vol. 36, pp. 209–230.

Dawe, R. A., Wheat, M. R., and Biener, M. S., 1992, "Experimental Investigation of Capillary Pressure Effects on Immiscible Displacement in Lensed and Layered Porous Media," *Transp. Porous Media*, Vol. 7, pp. 83–101.

Garboci, E. J., Bentz, D. P., and Martys, N. S., 1999, "Digital Images and Computer Modeling," in *Experimental Methods in the Physical Sciences 35, Method in the Physics of Porous Media*, Academic Press, San Diego, CA, Chap. 1, pp. 1–41.

Gottlieb, J. and Du Chateau, P., Eds., 1996, "*Parameter Identification and Inverse Problems in Hydrology, Geology, and Ecology*," Kluwer Academic Publishers, Dordrecht; Boston.

Gonzalesz, R. C. and Woods, R. E., 2002, *Digital Image Processing* (2nd ed.), Prentice-Hall, Upper Saddle River, N.J.

Grenier, A., Schreiber, W., Brix, G., and Kinzelbach, W., 1997, "Magnetic Resonance Imaging of Paramagnetic Tracers in Porous Media: Quantification of Flow and Transport Parameters," *Water Resour. Res.*, Vol. 33, pp. 1461–1473.

Huang, W. E., Smith, C. C., Lerner, D. N., Thornton, S. F., and Oram, A., 2002, "Physical Modelling of Solute Transport in Porous Media: Evaluation of an Imaging Technique Using UV Excited Fluorescent Dye," *Water Res.*, Vol. 36, pp. 1843–1853.

Khalili, A., Basu, A. J., and Pietrzyk, U., 1998, "Flow Visualization in Porous Media via Positron Emission Tomography," *Phys. Fluids*, Vol. 10, pp. 1031–1033.

Macari, E. J., Parker, J. K., and Costes, N. C., 1997, "Measurement of Volume Changes in Triaxial Tests Using Digital Imaging Techniques," *Geotech. Test. J.*, Vol. 20, pp. 103–109.

Majors, P. D., Smith, D. M., and Davis, P. J., 1991, "Effective Diffusivity Measurement in Porous-Media via NMR Radial Imaging," *Chem. Eng. Sci.*, Vol. 46, pp. 3037–3043.

Montemagno, C. D. and Gray, W. G., 1995, "Photoluminescent Volumetric Imaging-A Technique for the Exploration of Multiphase Flow and Transport in Porous-Media," *Geophys. Res. Lett.*, Vol. 22, pp. 425–428.

Ogata, A. and Banks, R. B., 1961, "A Solution of the Differential Equation of Longitudinal Dispersion in Porous Media," *Geological Survey Professional Paper 411-A*, U.S. Govt. Printing Office, Washington, DC, A1-A7.

Park, D. J. and McNeil, P. A., 1996, "Positron Emission Tomography for Process Applications," *Meas. Sci. Technol.*, Vol. 7, pp. 287–296.

Rechenmacher, A. L. and Finno, R. J., 2004, "Digital Image Correlation to Evaluate Shear Banding in Dilative Sands," *Geotech. Test. J.*, Vol. 27, pp. 13–22.

Robbins, G. A., 1989, "Methods for Determining Transverse Dispersion Coefficients of Porous-Media in Laboratory Column Experiments," *Water Resour. Res.*, Vol. 25, pp. 1249–1258.

Russ, J. C., 1994, *The Image Processing Handbook*, CRC Press, Cleveland, OH.

Selvadurai, A. P. S. and Dong, W., 2005, "A Time-Adaptive Scheme for the Solution of the Advection Equation With a Transient Flow Velocity," *Computer Modeling in Engineering and Sciences* (accepted).

Shattuck, M. D., Behringer, R. P., Johnson, G. A., and Georgiadis, J. G., 1997, "Convection and Flow in Porous Media. Part 1. Visualization by Magnetic Resonance Imaging," *J. Fluid Mech.*, Vol. 332, pp. 215–245.

Sun, N-Z., 1994, *Inverse Problem in Groundwater Modeling*, Kluwer Academic, Dordrecht.

Theodoropoulou, M. A., Karoutsos, V., Kaspiris, C., and Tsakiroglou, C. D., 2003, "A New Visualization Technique for the Study of Solute Dispersion in Model Porous Media," *J. Hydrol.*, Vol. 274, pp. 176–197.

Warner, G. S., Nieber, J. L., Moore, I. D., and Gesie, R. A., 1989, "Characterizing Macropores in Soil by Computed Tomography," *Soil Sci. Soc. Am. J.*, Vol. 53, pp. 653–660.